Observation of the fine structure for rovibronic spectral lines in the visible part of emission spectra of D_2

B. P. Lavrov,* I. S. Umrikhin, and A. S. Zhukov
Faculty of Physics, St. Petersburg State University, Sankt Petersburg 198504, Russia
(Received 21 March 2012; published 9 May 2012)

We have observed pseudodoublets representing a partly resolved fine structure of rovibronic lines in the visible part of the D_2 emission spectrum. They are characterized by splitting values of about 0.2 cm^{-1} and relative intensity of the doublet components close to 2.0. It is shown that they are determined by triplet splitting in lower rovibronic levels of various $^3\Lambda_g^{\pm} \rightarrow c^3\Pi_u^-$ electronic transitions. It is proposed to use the existence of such partly resolved fine-structure patterns for identification of numerous unassigned spectral lines of the D_2 molecule coming from a great variety of triplet "gerade" electronic states to vibrorotational levels of the $c^3\Pi_u^-$ state.

DOI: 10.1103/PhysRevA.85.052505 PACS number(s): 33.15.Mt, 33.20.Kf, 33.15.Pw

I. INTRODUCTION

The present paper reports observations concerning triplet-triplet electronic-vibrorotational (rovibronic) spectral lines in the visible part of the emission spectrum of the D_2 molecule. There are several peculiarities of the current knowledge of triplet rovibronic states and radiative transitions between them, which makes it possible to consider this knowledge insufficient and which motivated our experimental studies.

Most of the spectral lines in the visible and near-infrared parts of the emission spectrum of molecular deuterium are not yet classified. Thus, for example, in the latest compilation of experimental data [1], the working list of 27 488 recorded lines (within the wavelength ranges $\approx$309 − 1192 and 1647 − 2780 nm) contains only 8243 assignments. In our opinion, it is difficult to consider such a situation to be normal for an isotopomer of the simplest neutral molecule (four-particle quantum system).

Almost all of the experimental data on wave numbers for triplet rovibronic transitions of D_2 (3117 lines in Ref. [1]) were obtained by means of a traditional technique—photographing an image located in a focal plane of long-focus spectrographs.[1] The only exceptions are wave numbers of the 81 rovibronic lines in Ref. [2] and 3 lines in Ref. [3] obtained in middle IR (about 4.5 μm) by FTIR (Fourier transform infrared) and laser spectroscopy.

In contrast to the H_2 spectrum where both fine structures (FS) and hyperfine structures (HFS) of triplet lines and levels were studied for many electronic states and by various methods (see, e.g., the bibliography in Ref. [4]), for the D_2 molecule only fragmentary data concerning only FS were obtained, namely, fine-structure splitting values for 11 rovibronic levels of the $d^3\Pi_u^-$ state measured by the MOMRIE (microwave optical magnetic resonance induced by electrons) method [5]; pseudodoublets of partly resolved triplet structure for 18 of 81 recorded triplet lines in Ref. [2]; and completely resolved FS for 3 rovibronic lines in Ref. [3].

Most complete sets of data concerning wave-number values in visible and near IR together with empirical values of rovibronic energy levels were reported in Ref. [6] for the H_2 and in Ref. [1] for the D_2 molecules. They are based on the experimental results of Dieke and coworkers first reported in Ref. [7]. Describing his experimental setup in Ref. [7], Dieke mentioned that "in the low-pressure, low-temperature discharge the lines are considerably sharper, and for instance, the pseudodoublet structure of the $2p^3\Pi$ state which is about 0.2 cm^{-1} is well resolved under these conditions. This requires a resolving power of 100 000 in the visible." But in later compilations of the data for both H_2 [6] and D_2 [1] isotopomers, the fine structure of lines and empirical rovibronic energy levels was not mentioned at all. Moreover, in both cases the reported values of experimental errors ("a few hundredths cm^{-1}" for H_2 [6] and 0.05 cm^{-1} for D_2 [1]) are about one order of magnitude smaller than splitting in partly resolved fine structure earlier reported in Ref. [8] and mentioned in Ref. [7]. It is unclear how empirical rovibronic energy values were obtained with such precision when the more pronounced effect of the FS splitting was not taken into account.

There is noticeable asymmetry in studies of visible and near-IR spectra of light (H_2) and heavy (D_2) isotopomers of the hydrogen molecule. The FS of the H_2 spectral lines was discovered by Richardson and Williams as early as 1931 [9], exactly in the visible part of the spectrum (see also Ref. [8]). Although both isotopomers should have similar values of the FS splitting, its observation in the visible spectrum of the D_2 molecule was not reported in the literature known to the authors.

The goal of the present work was to study the opportunity of resolving the fine structure in the visible spectrum of the D_2 molecule by means of a spectroscopic technique developed in Refs. [10–12]. It is based on achieving a certain level of *optical resolution* of a spectrograph, recording spectral intensity distributions by matrix photoelectric detector, and by numerical deconvolution (inverse to the convolution operation) of recorded spectra. In dense multiline rovibronic spectra of H_2 and D_2 molecules, actual *digital resolution* achievable by

*lavrov@pobox.spbu.ru

[1]Nonlinear response of photographic recording does not ensure precise and reliable measurements of intensity distributions along the dispersion direction. It leads to the occurrence of systematic errors in evaluation of wave-number values of blended lines [10,11]. This is a widespread situation in rather dense multiline spectra of molecular hydrogen isotopomers having low mass and large Doppler profiles (e.g., about 20% of the D_2 triplet lines in [1]).

our technique could be much higher than optical resolution of a spectrometer which is limited not by its resolving power but by large Doppler broadening of spectral lines (see below). Thus it is possible to speak about some kind of sub-Doppler high-resolution spectroscopy.

II. EXPERIMENTAL

The spectroscopic part of our experimental setup was described in Ref. [12]. The 2.65-m Ebert-type spectrograph with an 1800-line/mm diffraction grating 100 mm wide was equipped with an additional camera lens and a computer-controlled CMOS matrix detector [22.2×14.8 mm^2, 1728×1152 triples of the red, green, and blue (RGB) photo detectors].[2] The calibrated spectrometer makes it possible, in the fully automatic regime, to record sets of individual windows (sections of a spectrum about 1.6 nm wide) at the experimentalist's discretion, or survey spectra by measuring sequences of successive windows with a specified overlap. Thus we obtained a digital automatic spectrometer with the following characteristics: effective focal length about 7 m and linear dispersion 0.077–0.065 nm/mm (for the wavelength region 400–700 nm). Maximal optical resolving power (up to 180 000) was achieved in resolving HFS components of Hg lines 546.1 and 404.6 nm, the FWHM of the instrumental profile for those wavelengths being 0.021 and 0.028 cm^{-1}, respectively.

When the entrance slit is uniformly illuminated, signals of one type of photo detector (B, G, or R) located in the same vertical column carry information concerning the brightness of the radiation at the same wavelength. Averaging makes it possible to increase the sensitivity of the spectrometer and the signal-to-noise ratio (SNR) for data obtained by a single exposure. To reach the required value of the SNR, we made many records (up to 150 shots for the same wavelength fragment and the same discharge conditions). The averaging of those results made it possible to reach a SNR value up to 10^4 (see Ref. [12]).

For recording the D_2 spectra with low resolution, high sensitivity, and a large population of high rotational levels, we used a hot-cathode capillary-arc discharge lamp LD-2D described in Ref. [13] (pure D_2 under pressure $\approx$6 Torr, capillary inner diameter 2 mm, current density $\approx$10 A/cm^2). Gas temperature $T = 1890 \pm 170$ K was obtained from the intensity distribution in the rotational structure of the $(2-2)\,Q$ branch of the Fulcher-α band system (see, e.g., Refs. [14,15]). It corresponds to Doppler linewidths (FWHM) $\Delta\nu_D = 0.22$–0.37 cm^{-1} for $1/\nu = 420$–700 nm. Therefore we were able to open the entrance slit of the spectrometer up to 60 μm to gain more signal (and corresponding decrease in data accumulation time) without significant loss in resolution.

To achieve the best possible optical resolution we have to decrease Doppler broadening by diminution of the gas temperature in plasma. It is obviously favorable for increasing spectral resolution, but lowering the temperature automatically leads to lower population densities of high rotational levels in ground and excited electronic states and to much smaller intensities of corresponding spectral lines. Therefore we had to use some compromised plasma conditions. Thus in high-resolution experiments we used glow discharge with cold cathode and water-cooled walls. An additional third electrode with an axial cylindrical hole diameter of 4 mm was located on discharge axes between a cathode and an anode. Through a hole in an anode, the flux of radiation emitted by plasma inside additional electrode was focused on the entrance slit of the spectrometer. With this geometry we achieved current density as low as 0.4 A/cm^2 and $T = 610 \pm 20$ K.

It should be emphasized once more that up until now, the overwhelming majority of the data on the wave numbers for rovibronic transitions of the D_2 molecule have been obtained by photographic recording of spectra (see, e.g., Refs. [16,17]). Our way of determining wave-number values is based on the linear response of the CMOS matrix photo detector on the spectral irradiance and digital intensity recording. Both of these factors provide an extremely important advantage for our technique over traditional photographic recording with microphotometric or visual comparator reading. It not only makes it easier to measure the relative spectral line intensities but also makes it possible to investigate the shape of the individual line profiles and, in the case of overlap of the contours of adjacent lines (so-called blending), to carry out numerically the deconvolution operation and thus to measure the intensity and wavelength of blended lines. As is well known, it is this blending that makes it very hard to analyze dense multiline spectra of the D_2 molecule [1].

We treat the problem of wave-number determination as that of conditional optimization: parametrization of a model for an intensity distribution and determination of an optimal set of parameters by searching a global minimum of an objective function under specified conditions. Thus for small regions of the spectrum ($\approx$0.5 nm wide, about one-third of a window, containing 500–600 vertical columns of photodetectors; see Fig. 1) the observed spectral intensity distribution (dependence of the photoelectric signal of the kth photodetector I_k^{expt} on the detector position x_k) was approximated by a superposition of a finite number M of line profiles $f_i(x)$ with a width Δx common for all lines within an analyzed region:

$$I^{\text{calc}}(x) = I_{\text{bg}} + \sum_{i=1}^{M} A_i f_i\left(x, x_i^0, \Delta x\right), \tag{1}$$

where I_{bg} is a constant background intensity and A_i is the amplitude of the ith profile (intensity in the line center x_i^0).

We used an objective function in the form of a sum of squares of deviations between experimental and "synthesized" intensity distributions,

$$\Phi\left(\left\{A_i, x_i^0\right\}_{i=1\cdots M}, \Delta x, I_{\text{bg}}\right) = \sum_{k=1}^{K} \left[I_k^{\text{expt}} - I^{\text{calc}}(x_k)\right]^2, \tag{2}$$

where K indicates a number of experimental intensity values I_k^{expt} in the spectral region under the study.

If the experimental errors of the I_k^{expt} values are random and distributed according to a normal (Gaussian) law, the solution obtained by the least-squares criterion for (2)

[2]Actually, every pixel of the matrix contains four RGGB detectors, but one from two identical G photodetectors was not used for recording of spectra.

corresponds to the maximum likelihood principle. For determining a global minimum of the objective function (2) in multidimensional parameter space we used a special computer program based on Levenberg-Marquardt's algorithm [18,19].

Our studies showed that in HFS of Hg spectral lines [12] and in the low-resolution experiments, approximation of line profiles by Gaussian function $f_i(x) = \exp(-\frac{1}{2}[x - x_i^0]^2/\Delta x_G^2)$ (with the linewidth Δx_G) was adequate, providing random scatter of the $I_k^{\text{expt}} - I^{\text{calc}}(x_k)$ deviations and sufficiently high accuracy.

The analysis of line profiles obtained in high-resolution experiments showed that Gaussian function is insufficient, and we had to use more flexible Voigt profiles:

$$f_i(x) = \frac{\int_{-\infty}^{+\infty} \frac{\exp(-t^2)}{\left(\frac{\Delta x_L}{\sqrt{2}\Delta x_G}\right)^2 + \left(\frac{x - x_i^0}{\sqrt{2}\Delta x_G} - t\right)^2} dt}{\int_{-\infty}^{+\infty} \frac{\exp(-t^2)}{\left(\frac{\Delta x_L}{\sqrt{2}\Delta x_G}\right)^2 + t^2} dt}, \tag{3}$$

where Δx_L denotes Lorentzian linewidth.

The values for all the $2M + 3$ parameters ($\{A_i, x_i^0\}_{i=1\cdots M}$, Δx_G, Δx_L, and I_{bg}) obtained by minimizing (2) are optimal for the observed intensity distribution under the condition of identical Δx_G and Δx_L values for all the lines. Thus it is possible to obtain optimal values of the amplitude and a line

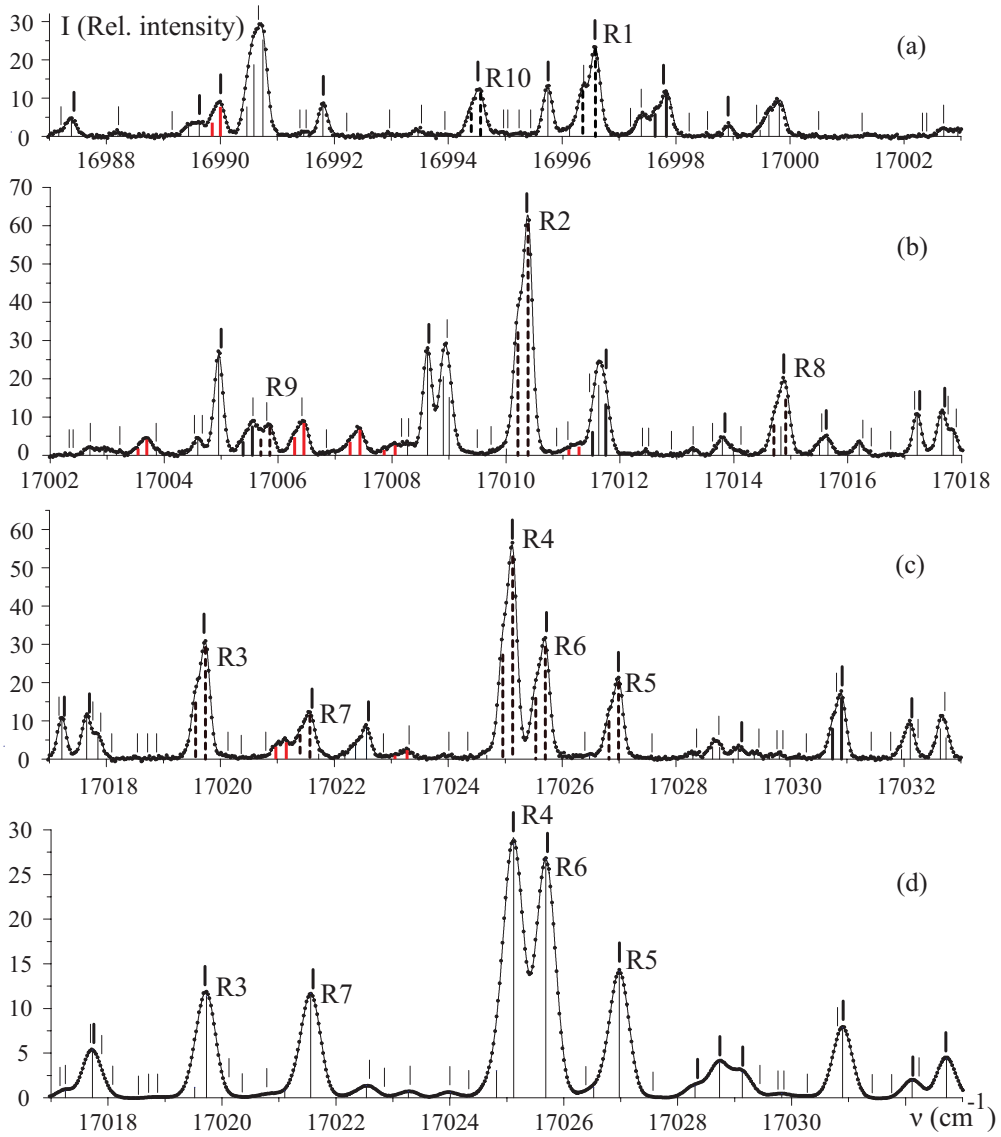

FIG. 1. (Color online) Part of the D_2 spectrum containing the first 10 lines of the R branch for the $(1-1)$ band of the $i^3\Pi_g^- \rightarrow c^3\Pi_u^-$ electronic transition obtained in high- [(a)–(c)] and low- (d) resolution experiments. Experimental data I_k^{expt} in relative units are indicated by dots. Solid lines represent the intensity distribution calculated as a sum of optimal Voigt profiles. Wave-number values reported in Ref. [1] are marked by short vertical line segments above I_k^{expt}; those displayed in bold were used for calibration of our spectrometer. Spectral lines obtained by the deconvolution are presented as "stick diagrams" indicating their wave-number positions ν_i^0 and amplitudes A_i. Pairs of sticks displayed in bold represent the pseudodoublets having specific characteristics (see text).

center for each spectral line as well as a common value of the total "observed" linewidth Δx calculated from optimal values of Δx_G and Δx_L.

In the case of long-focus spectrometers the dependence of the wavelength on the coordinate along the direction of dispersion is close to linear in the vicinity of the center of the focal plane. It can be represented as a power series expansion over of the small parameter x/F (the x coordinate represents a small displacement from the center of the matrix detector, and F is the focal length of the spectrometer), which in our case does not exceed 2×10^{-3} [12]. On the other hand, the wavelength dependence of the refractive index of air $n(\lambda)$ is also close to linear inside a sufficiently small part of the spectrum. Thus, when recording narrow spectral intervals, the product $\lambda_{\text{vac}}(x) = \lambda(x)n(\lambda(x))$ has the form of a power series of low degree. This circumstance makes it possible to calibrate the spectrometer directly in vacuum wavelengths $\lambda_{\text{vac}} = 1/\nu$, thereby avoiding the technically troublesome problem of accurate measuring of the refractive index of air for various experimental conditions. For spectrometer calibration the experimental vacuum wavelength values $(1/\nu)$ of bright, nonblended D_2 lines from Ref. [1] were used as the standard reference data.[3] They show small random spread around a smooth curve representing dependence of the wavelengths on positions of corresponding lines in the focal plane of the spectrometer. Moreover, these random deviations are in good accordance with normal distribution. Thus it is possible to obtain precision for new wave-number values better than that of the reference data due to smoothing. The calibration curve of the spectrometer was obtained by polynomial least-squares fitting the data with accuracy better than 2×10^{-3} nm.

III. RESULTS AND DISCUSSION

Following the method described above we measured the D_2 spectra in low- and high-resolution experiments for wave-number regions 14 378.80–23 894.65 cm^{-1} (695–418 nm) and 15 948.82–18 331.28 cm^{-1} (627–545 nm) [20], respectively. Within these intervals, 11 986 and 3518 spectral lines were distinguished after the deconvolution. Detailed analysis of the data will be reported in subsequent papers. In the present paper we shall restrict ourselves to consideration of one particular but rather typical case, which allows us to illustrate some general features of our first observations.

As an example, four fragments of the D_2 spectrum containing the first 10 lines of the R branch for the $(1-1)$ band of the $i^3\Pi_g^- \rightarrow c^3\Pi_u^-$ electronic transition are shown in Fig. 1. The first fragments [(a), (b), and (c)] are three parts of the same window recorded in the high-resolution experiment (discharge current $I = 30$ mA, entrance slit $\Delta S = 15$ μm, observed FWHM $\Delta\nu = 0.18\ \text{cm}^{-1}$). They were used separately in the deconvolution procedure described above. The fourth fragment (d) is identical to the third one (c), but it was obtained in a low-resolution experiment ($I = 300$ mA, $\Delta S = 60$ μm, $\Delta\nu = 0.39\ \text{cm}^{-1}$). One may see that two identical fragments measured with different spectral resolution are qualitatively different. In the low-resolution case, all lines look like singles with symmetrical profiles. In high-resolution experiments, the partly resolved fine structure of some of the lines becomes apparent as asymmetry of their profiles, although some other lines remain single with symmetric profiles [see Figs. 1(a) and 1(b)]. This is a result of, say, optical resolution only. The deconvolution of measured intensity distributions based on the numerical optimization technique described above provides an opportunity to recognize narrow substructures within observed asymmetric profiles. The results of such digital resolution are shown in Fig. 1 as "stick diagrams" of the individual components, indicating their wave-number positions ν_i^0 and amplitudes A_i. Numerical data concerning the $(1-1)$ R-branch lines under the study are also presented in Table I. One may see from the table that in our conditions this technique is able to provide high enough precision in wave numbers and relative intensities of latent spectral lines. Moreover, additional resolving power obtained by the deconvolution is sufficiently higher than that corresponding to Rayleigh criterion.

Among the many lines shown in Figs. 1(a), 1(b), and 1(c), the 22 pairs of recognized lines (sticks) catch one's eye because they have distinguishing features: the splitting value is about 0.2 cm^{-1} and intensity ratios of the violet (strong) and red (weak) components are close to 2.0. The sticks representing such pseudodoublets are shown in bold. Ten of them (displayed as black dashed sticks) were previously classified as single rovibronic lines belonging to the $(1-1)$ R branch of the $i^3\Pi_g^- \rightarrow c^3\Pi_u^-$ electronic transition [1]. Four other cases (displayed in solid black) were also classified as triplet lines coming to vibrorotational levels of the $c^3\Pi_u^-$ state [1]. Recently these assignments were confirmed by statistical analysis of the experimental wave numbers in the framework of Rydberg-Ritz combination principle [10]. Eight other pairs (displayed in grey (red online)) are not assigned so far.

The splitting values obtained in present work for the $(1-1)$ R-branch lines are shown in Fig. 2 together with analogous data obtained in middle IR for the $a^3\Sigma_g^+ \rightarrow c^3\Pi_u^-$ transitions of D_2. One may see that the results obtained from two different band systems having common $c^3\Pi_u^-, v'' = 1, N''$ rovibronic states are in good agreement. Moreover, as observed in both experiments with the D_2 molecule, the wave-number splittings are almost the same as the pseudodoublet splitting of the FS sublevels of the $c^3\Pi_u^-, v'' = 1, N'' = 2,4$ levels of the H_2 molecule.

Thus it is natural to interpret all observed pseudo doublets as partly resolved FS patterns of the ${}^3\Lambda_g^{\pm}, v', N' \rightarrow c^3\Pi_u^-, v'', N''$ rovibronic transitions mainly determined by FS splitting of rovibronic levels in the $c^3\Pi_u^-$ state. Here Λ is the quantum number for projection of electronic orbital angular momentum onto internuclear axes, v denotes vibrational quantum number, N denotes the quantum number of total angular momentum excluding electron and nuclear spins, and upper

[3] Our previous studies [12] of the emission spectrum of capillary-arc discharge lamp analogous to that described in [22] but filled with the $D_2 + H_2 + Ne$ gas mixture show that wave-number values of atomic lines of Ne [23] and those of bright nonblended lines of the H_2 [6] and D_2 [1] molecules are in rather good mutual accordance and may be used as reference data for spectrometer calibration, providing an accuracy of about 10^{-3} nm [20].

TABLE I. Wave-number values (in cm^{-1}) and relative intensities I_S/I_W for strong and weak components for pseudodoublets of the R-branch lines for the $(1-1)$ band of the $i^3\Pi_g^- \rightarrow c^3\Pi_u^-$ electronic transition [the T- 3e-2c (1-1) RN" rovibronic transitions in Dieke notation [1]]. The ν_S and ν_W are wave numbers of strong and weak components; $\Delta\nu_{SW} = \nu_S - \nu_W$; $\Delta\nu_{LR}$ indicates the wave numbers obtained in low-resolution experiments. Experimental error (one standard deviation) is shown in brackets in units of the last significant digit.

Reference [1]		Present work			
Assignment	ν	ν_{LR}	ν_S, ν_W	$\Delta\nu_{SW}$	I_S/I_W
T- 3e-2c (1-1) R1	16996.58	16996.57(2)	16996.58(3)s	0.22(5)	1.93(5)
	16996.38	16996.31(2)	16996.36(4)w		
T- 3e-2c (1-1) R2	17010.36	17010.37(2)	17010.39(3)s	0.18(4)	1.88(2)
			17010.21(3)w		
T- 3e-2c (1-1) R3	17019.71	17019.73(2)	17019.74(3)s	0.17(5)	1.99(4)
			17019.57(4)w		
T- 3e-2c (1-1) R4	17025.11	17025.12(2)	17025.13(3)s	0.17(4)	1.94(3)
			17024.96(3)w		
T- 3e-2c (1-1) R5	17026.97	17026.98(2)	17026.99(3)s	0.17(5)	2.05(7)
			17026.82(4)w		
T- 3e-2c (1-1) R6	17025.71	17025.69(2)	17025.70(3)s	0.17(5)	1.84(4)
			17025.53(4)w		
T- 3e-2c (1-1) R7	17021.60	17021.56(2)	17021.57(4)s	0.18(6)	1.82(11)
			17021.40(4)w		
T- 3e-2c (1-1) R8	17014.87	17014.88(2)	17014.91(4)s	0.21(6)	1.90(60)
			17014.70(4)w		
T- 3e-2c (1-1) R9	17005.79	17005.82(2)	17005.86(4)s	0.16(6)	1.80(20)
			17005.70(5)w		
T- 3e-2c (1-1) R10	16994.53	16994.54(2)	16994.57(4)s	0.16(6)	1.89(14)
			16994.40(4)w		

and lower states are marked by single and double primes, respectively.

The intensity ratios I_s/I_w for the $(1-1)$ R-branch lines under the study are listed in Table I. These values cannot be compared with any other experimental results because they were not reported in the literature known to us. At the same time one may see that our experimental values are close to 2.0. Exactly this value may be obtained by the well-known Burger-Dorgello-Ornstein sum rule for intensities within narrow multiplets when one assumes that the triplet splitting in upper rovibronic states may be neglected while in the lower rovibronic states $c^3\Pi_u^-, v = 1, N''$ two fine-structure sublevels ($J'' = N'' - 1$ and $J'' = N'' + 1$) are close to each other and located noticeably lower than that with $J'' = N''$.[4] These assumptions are in agreement with IR tunable laser observations ($E_{J''=2} \approx E_{J''=0} < E_{J''=1}$) for the fine structure of the $a^3\Sigma_g^+, v' = 4, N' = 3 \leftarrow c^3\Pi_u^-, v'' = 3, N'' = 1$ rovibronic transition reported in Ref. [3]. Thus our ability to measure both the intensities and splitting values gives us an opportunity to get information about an order and separation of the fine-structure sublevels.

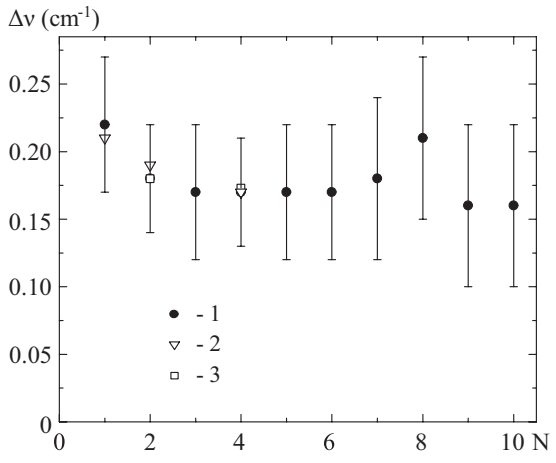

FIG. 2. Values of the splitting in pseudodoublets observed in the present work for the $i^3\Pi_g^-, v' = 1, N'' + 1 \rightarrow c^3\Pi_u^-, v'' = 1, N''$ rovibronic transitions of D_2 (points 1) and those for the $a^3\Sigma_g^+, v' = 2, N'' \rightarrow c^3\Pi_u^-, v'' = 1, N''$ transitions of D_2 obtained by FTIR spectroscopy in [2] (points 2). 3 indicates the splitting values in pseudodoublets of the $c^3\Pi_u^-, v = 1, N = 2,4$ rovibronic levels of the H_2 molecule, calculated from the data reported in Ref. [21].

Finally, two main results of our observations may be formulated as follows. The deconvolution of intensity distributions recorded by a matrix photoelectric detector by means of numerical optimization procedure is a powerful tool for determining wave numbers and intensities of substructures within apparent line profiles masked by overlapping of adjacent lines (blending) and line broadening in traditional photographic recording of spectra. In contrast to fragmentary

[4]There are six possible sequence orders of FS sublevels leading to formation of visible pseudodoublet structure of lines and levels. Only one of them formulated above provides the intensity ratio $I_s/I_w = 2.0$. The four other orders give strong dependence of the I_s/I_w value on N'', and another one gives $I_s/I_w = 1/2$.

results of tunable laser techniques, such Doppler-free classic spectroscopy is able to provide huge volumes of data for broad regions of molecular spectra. It should be stressed that we are working in the visible part of the spectrum, most suitable for various applications. Even partly resolved fine structure of spectral lines provides an opportunity to expand the existing identification of triplet rovibronic lines by detecting those doublets in experimental spectra. The doublets analyzed above are especially promising because they are easily recognizable in the spectrum due to their distinguishing features. Within the spectral region under the study (545–627 nm) we already found more than 200 pairs of unassigned lines which may represent pseudodoublets of partly resolved FS of rovibronic transitions between $^3\Lambda_g^{\pm}$ and $c^3\Pi_u^-$ electronic states of the D_2 molecule [20].

ACKNOWLEDGMENTS

The authors are indebted to S. C. Ross for providing an electronic version of Appendix C from Ref. [1]. The present work was supported, in part, by the Russian Foundation for Basic Research, Grant No. 10-03-00571-a.

[1] R. S. Freund, J. A. Schiavone, and H. M. Crosswhite, J. Phys. Chem. Ref. Data. **14**, 235 (1985).
[2] I. Dabrowski and G. Herzberg, Acta Phys. Hung. **55**, 219 (1984).
[3] P. B. Davies, M. A. Guest, and S. A. Johnson, J. Chem. Phys. **88**, 2884 (1988).
[4] L. Jozefowski, C. Ottinger, and T. Rox, J. Mol. Spectrosc. **163**, 414 (1994).
[5] R. S. Freund and T. A. Miller, J. Chem. Phys. **59**, 4073 (1973).
[6] H. M. Crosswhite, ed., *The Hydrogen Molecule Wavelength Tables of G. H. Dieke* (Wiley, New York, 1972).
[7] G. H. Dieke, J. Mol. Spectrosc. **2**, 494 (1958).
[8] E. W. Foster and O. W. Richardson, Proc. R. Soc. London A **189**, 175 (1947).
[9] O. W. Richardson and W. E. Williams, Nature **127**, 481 (1931).
[10] B. P. Lavrov and I. S. Umrikhin, J. Phys. B **41**, 105103 (2008).
[11] B. P. Lavrov and I. S. Umrikhin, Rus. J. Phys. Chem. B **3**, 397 (2009).
[12] B. P. Lavrov, A. S. Mikhailov, and I. S. Umrikhin, J. Opt. Technol. **78**, 180 (2011) .
[13] V. S. Greben'kov, B. P. Lavrov, and M. V. Tyutchev, Sov. J. Opt. Technol. **49**, 115 (1982).
[14] B. P. Lavrov, Opt. Spectrosc. **48**, 375 (1980).
[15] S. A. Astashkevich, M. Kaning, E. Kaning, N. V. Kokina, B. P. Lavrov, A. Ohl, and J. Ropcke, J. Quantum Spectrosc. Radiat. Transfer **56**, 725 (1996).
[16] M. Roudjane, F. Launay, and W.-U. L. Tchang-Brillet, J. Chem. Phys. **125**, 214305 (2006).
[17] M. Roudjane, W.-U. L. Tchang-Brillet, and F. Launay, J. Chem. Phys. **127**, 054307 (2007).
[18] K. Levenberg, Q. Appl. Math. **2**, 164 (1944).
[19] D. Marquardt, SIAM J. Appl. Math. **11**, 431 (1963).
[20] B. P. Lavrov and I. S. Umrikhin, e-print arXiv:1112.2277v1.
[21] L. Jozefowski, C. Ottinger, and T. Rox, J. Mol. Spectrosc. **163**, 398 (1994).
[22] B. P. Lavrov and L. P. Shishatskaya, Sov. J. Opt. Technol. **46**, 692 (1979).
[23] E. B. Saloman and C. J. Sansonetti, J. Phys. Chem. Ref. Data **33**, 1113 (2004).